

Very low frequency ambient noise at the seafloor under the Beaufort Sea icecap

Spahr C. Webb

Scripps Institution of Oceanography, University of California, San Diego, La Jolla, California 92093

Adam Schultz

School of Oceanography, University of Washington, Seattle, Washington 98195

(Received 10 May 1991; accepted for publication 29 October 1991)

The first results from a deployment of four instruments on the floor of the Beaufort Sea in March 1990 are presented. The instruments recorded pressure fluctuations in the band from 0.0005 to 8 Hz during a 2-week period. The pressure spectra derived from these measurements show very low energy in the microseism peak near 0.1 Hz in comparison with measurements from the Pacific or Atlantic seafloor. The microseism band shows a series of spectral peaks and valleys likely associated with the modes of the ocean-seafloor Rayleigh wave waveguide. The shape of the microseism peak is remarkably stable during the experiment although the amplitude varies by about 10 dB. The signals are very coherent between adjacent instruments and suggest propagation in the microseism band from a source in the Gulf of Alaska. The pressure spectra rise rapidly toward lower frequency below 0.02 Hz, but Arctic spectra are less energetic than spectra from sites on either Pacific or Atlantic seafloors at all frequencies. The long period energy appears to be related to flexural-gravity waves on the ocean surface. The pressure measurements predict amplitudes for these waves in general agreement with previous tilt and displacement measurements made on the ice.

PACS numbers: 43.30.Nb, 43.30.Ma

INTRODUCTION

Four instruments were deployed through the polar ice in March 1990 to record pressure fluctuations in the band from 0.0005 to 8 Hz on the floor of the Beaufort Sea. The instruments were left on the seafloor from 16 March 1990 through 6 April 1990 and collected a continuous record of pressure fluctuations during the first 14 days of the experiment. The measurements later proved to be sensor noise limited above 2 Hz. As far we know this is the first long record of low-frequency noise obtained on the Arctic seafloor. Pressure spectra from the seafloor in the Atlantic or the Pacific Ocean invariably show a pronounced peak between 0.1 and 5 Hz usually called the "microseism" peak.^{1,2} The origin of this energy is now well understood to be the result of seismoacoustic waves forced by nonlinear interaction of surface gravity waves (ocean waves) over the ocean surface. This mechanism generates elastic waves at double the frequency as that of the surface waves which are the source. A second smaller spectral peak at slightly lower frequency is usually also present. This peak is called the "single or primary frequency" microseism peak since these signals are driven directly by ocean waves and no frequency doubling occurs.³ The ice sheet prevents the growth and propagation of ocean waves over the Arctic ocean, eliminating these mechanisms as a source of low-frequency sound. A primary motivation in siting this experiment in the Arctic was to search for other sources of low-frequency sound besides the well studied wave-wave interaction mechanism. The shattering of ice during the movement of the ice sheet is also known to be an important intermittent source of sound at frequencies as low

as 10 Hz.⁴ Ice surface displacement and tilt measurements have detected oscillations of tens of seconds in period that might be detected with a pressure transducer on the deep-sea floor if of sufficiently long wavelength.

Several seismometer stations were established on the ice near the APLIS90 camp in conjunction with the pressure measurements. One seismometer station was also set up on the shores of the Beaufort Sea near Prudhoe Bay, Alaska for the duration of the experiment. This station will be used to monitor the component of the microseism wave field that propagates onto the continents. Microseisms are detected at seismic stations throughout all the continents. The seismic measurements will be discussed and compared with the seafloor pressure measurements in a subsequent paper.

I. PREVIOUS WORK

Milne *et al.* describe measurements of ambient noise at frequencies as low as 20 Hz from hydrophones towed across the Beaufort seafloor in 451 m of water.⁵ These measurements showed great variability in the noise levels near 20 Hz, but demonstrated that very low noise levels could be found at Arctic seafloor sites. Measurements at longer periods in the Arctic have been mostly restricted to measurements from hydrophones suspended from the ice.^{4,6-8} The pressure signal associated with low-frequency sound is greatly reduced at depths much less than one-half of a wavelength because of reflection at the free surface, and therefore suspended hydrophones are probably useless for the study of sound below a few Hertz. Measurements obtained with hydrophones in midwater at low frequencies are dominated by

flow noise and cable strum. Lewis and Denner deployed an extensive array of drifting buoys to map acoustic signal levels in the Beaufort Sea.^{7,8} They report an inertial period fluctuation in acoustic levels at 3.2 and 10 Hz, indicative of flow and strum noise. This problem was most severe during the summer months when the rate of drift was the fastest. Data from the winter months were less affected by flow noise. The Lewis and Denner study provides the most complete record of long-term variability and spatial coherence of low-frequency sound in the Beaufort Sea.

We found only one example in the literature of seismic instruments deployed on the Arctic ocean floor to study signals below 1 Hz.⁹ Very low signal levels were found in the band from 0.1 to 1 Hz in short records obtained from three sites on the seafloor using an ocean bottom seismometer system tethered to the ice surface. Instrument noise predominated at lower frequencies. Only about 2.5 h of records were obtained during this experiment, but from these results the authors concluded the Arctic ocean floor was a very quiet location from which to record signals from distant earthquakes.

At the seafloor in either the Atlantic and Pacific ocean, the pressure spectrum is relatively energetic at frequencies below 0.03 Hz. Low-frequency ocean waves (infragravity waves) at these frequencies are of sufficiently long wavelength and energetic to overwhelm other sources of low-frequency pressure fluctuations. Infragravity waves may be generated at coastlines by a conversion through nonlinear processes from short period wave energy (wind driven waves or swell) into long period waves.¹⁰ Since no waves break on Arctic shores in winter, one would expect this source of low-frequency pressure fluctuations to be absent in the Arctic. However, several groups of researchers have deployed long period seismometers (or gravimeters) on the Arctic ice and detected oscillations primarily in the band from 0.017 to 0.05 Hz (periods from 20–60 s).^{11–13} These motions are also detected on strain gauges and tiltmeters deployed on the ice.^{14,15} These distortions of the ice are either driven by the local wind, or propagate in from the open ocean. Some evidence of wavelike propagation has been seen in the on-ice measurements.

II. THE APLIS DEPLOYMENT

Four instruments were deployed through the ice at the 1990 APLIS ice camp on 16 March 1990 (Fig. 1). The instruments are designated by color: red, white, green, and blue. The four instruments were designed to fit easily through a 1-m-diam hole melted through the ice and to be transported in helicopters (Fig. 2). The pressure fluctuations were detected using a differential pressure gauge.¹⁶ The differential gauge has lower noise compared to conventional low-frequency hydrophones at frequencies below 0.1 Hz, although poorer performance above 1 Hz. The gauge has been used during a series of experiments directed at studying low-frequency sound in the ocean.^{1,17,18}

An 8088 microcomputer controlled the acquisition of data and drove the small (40 Mbyte) cartridge tape recorder used for recording. The instruments recorded pressure fluctuations sampled continuously at a 16-Hz rate. Tape capac-

ity was sufficient for a 14-day record at this rate. Timing was maintained by a temperature compensated quartz clock. The clock drift at the end of the record was precisely measured, and timing after correcting for drift is thought to be better than 20 ms over the 3-week period, with the exception of the instrument "red" because of a problem with the rubidium clock used to start the instruments. An EG&G model 8242 acoustic release/transponder permitted recovery of each instrument and enabled the instrument to be located under the ice.

The instruments were deployed through the same hole over a 4-h period on 16 March 1990. The ice sheet during this interval was drifting at a rate of nearly 500 m/h. The trajectory of the ice station determined the locations of the instruments on the bottom (Fig. 1). The direction of station drift changed slightly during the deployments. The instruments lie along a roughly 1.5 km long, gently curving arc with a spacing of about 500 m. The instruments were acoustically tracked during and after deployment using a long baseline acoustic array maintained by the Applied Physics Laboratory of the University of Washington. The relative instrument locations are known to better than a few meters. The positions were tied into latitude and longitude coordinates using global positioning system (GPS), and absolute locations are known to better than 100 m. We had originally planned to deploy a two-dimensional array, but the very fast drift of the ice during this period required greater synchronicity of the deployments than was thought possible at multiple remote sites.

The ice camp drifted in a large loop ending up about 15 km from the deployment site during the 3-week deployment. For a time, the camp was over 30 km from the deployment site. The instruments were released from the anchors by acoustic command on 5 April 1990. Flotation in the form of three glass balls brought each instrument to the surface. The instruments moved with the ice after release. The instruments were suspended 30 m below the ice by the flotation so that the acoustic transponder within each acoustic release could be heard by a hydrophone suspended through the ice despite deep ice keels between the hydrophone and the instruments. The instruments were located using several measurements of bearing and distance. Some ambiguous measurements were generated by reflections from nearby ice keels, but all the instruments were located within a 2-day period. Four 1-m-diam holes were melted through the ice and divers were able to quickly locate each instrument. The instruments were retrieved and flown back to camp on 7 April 1990. The timing was then checked against time maintained by a rubidium clock, and the tapes retrieved from the instruments. Three of the four instruments obtained complete records, the fourth ("white") stopped recording after 2 days.

III. THE MICROSEISM BAND

The spectra of pressure fluctuations measured at this site on the floor of the Beaufort Sea are very unenergetic in comparison to measurements from any site in the eastern Pacific or the western Atlantic Ocean (Fig. 3). We see very

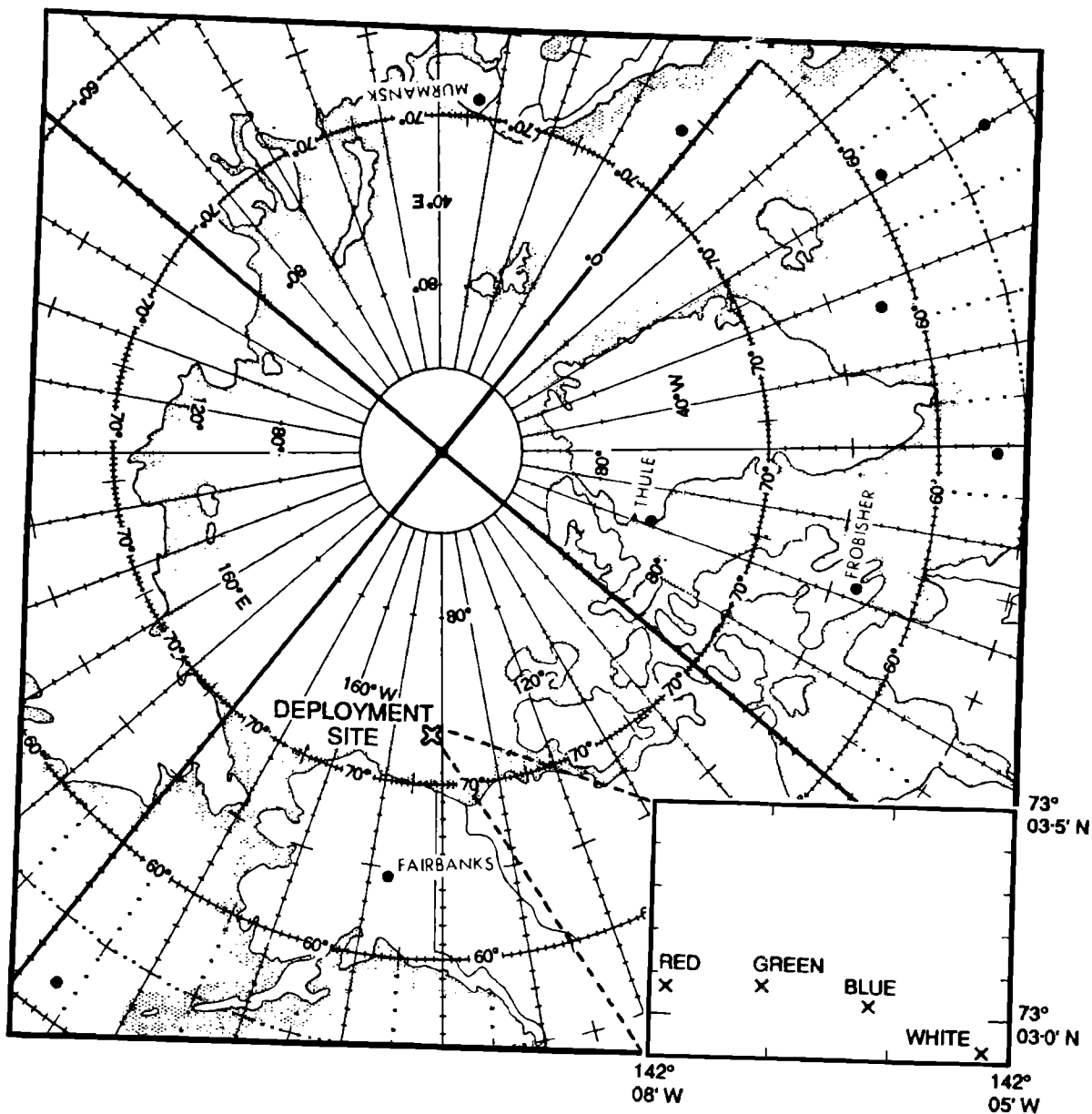


FIG. 1. The APLIS deployment site to the North of Prudhoe Bay, Alaska. Insert: locations of the four instruments within the array named by color.

small single and double frequency microseism peaks in the band from 0.08 to 1.2 Hz. There is a sharp rise toward very low frequency apparently associated with infragravity waves, but the energy at these frequencies is also much less than at any site on the Pacific seafloor. The low signal levels at this site reveal the electronic noise limit of the differential pressure gauges near 10^{-2} Pa²/Hz at 0.5 Hz and 10^{-3} Pa²/Hz above 1 Hz for the best instrument (Fig. 3). The spectra from the four instruments look virtually identical, and the data is coherent at all frequencies for which the signal level is above the noise (Fig. 4).

We had hoped to look for events associated with ice movement in the band above 1 Hz. The relatively high noise level in the differential pressure gauges surprised us, and allow us to remark only that no very energetic ice cracking

events appear to have occurred. Further data analysis may yield more extensive results. Buck and Wilson have reported ice cracking related noise levels near a ridge of 10^{-2} Pa²/Hz at 10 Hz during noisy intervals. Lewis and Denner also report noise levels at 10 Hz detected with drifting buoys as high as 10^{-2} Pa²/Hz during some intervals in the winter. Such events might be detected with the APLIS deployment instrumentation. Makris and Dyer report a broad peak around 15 Hz reaching 10^{-3} Pa²/Hz associated with ice cracking. Typical levels near 10 Hz during quiet intervals have been reported to be near 10^{-5} Pa²/Hz.¹⁹

In Fig. 4, we see a primary frequency microseism peak at 0.08 Hz, and a double frequency microseism peak that is further divided into a series of peaks at 0.15, 0.31, 0.54, 0.73, 0.95, and 1.16 Hz. The "single frequency microseism peak"

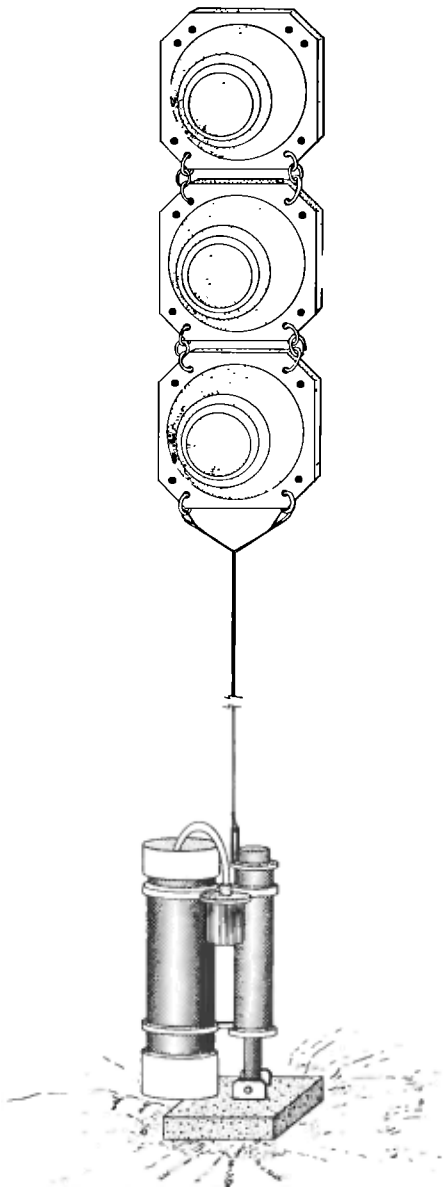


FIG. 2. The Arctic instrument as deployed on the seafloor. The glass spheres for flotation float 30 m above the instrument. Shown are the differential pressure gauge (small cylinder with cabling), the main pressure case for the recorder (largest cylinder) and the acoustic transponder/release over the 50-kg anchor. The instrument separates from the anchor for recovery.

is associated with Rayleigh waves energized by the pounding of ocean waves along the world's coastlines.³ The double frequency microseisms are created by nonlinear interaction of ocean waves in the open ocean and near the coasts.

The amplitude and shape of the microseism peak is remarkably stable over the duration of the experiment (Fig. 5). Measurements of the microseism energy from sites in the Pacific or the Atlantic vary from day to day by as much as 30 dB as the ocean wave climate varies. In contrast, the Arctic measurements show only about a 10-dB variation in the en-

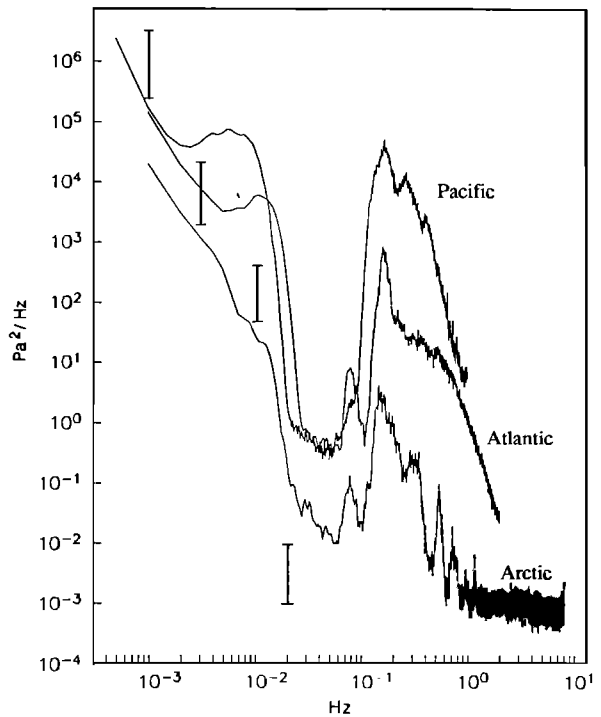


FIG. 3. Pressure spectrum from an Arctic instrument, showing the multiple microseism peaks and rising energy toward very low frequencies associated with flexural-gravity waves (infragravity waves). Four bars refer to a range of estimates of the pressure spectrum inferred from tilt measurements from the ice in the Norwegian Sea.¹⁴ Also shown, pressure spectra from sites in the Atlantic and Pacific Oceans.

ergy in the microseism peak during the experiment with the exception of an interval affected by wave trains from two large earthquakes (Fig. 6). The energy varies on time scales on the order of a few days, which is typical of ocean storms. At other sites, the microseism spectrum varies in concert with changes in the local ocean wave spectrum, but there is persistent low-frequency component of the microseism wave field associated with distant storms over the ocean.^{1,20} The ocean wave field evolves toward lower frequency and larger waves under a persistent wind. The spectrum of the swell may shift with time toward shorter period and smaller waves as a consequence of dispersion (waves from distant storm sources). These types of evolution of the wave field are often apparent in the seafloor microseism spectra as well, with slow shifts in frequency of peaks in the microseism spectra on the time scale of a few days. In contrast, no long term shifts in the frequency of individual peaks are evident in the Arctic data. The arctic microseism signal is probably "tele-seismic" and caused by ocean waves over a broad area of the world's oceans. The day to day variability of the ocean wave field may be obscured by averaging over a large area. The multiple peaks in the spectrum appear unrelated to the ocean wave spectrum.

Occasional, large earthquakes generate long-lived wave trains that are very apparent in the spectral record as large peaks centered around a 25-s period (Fig. 5). The most prominent event is a sequence of two earthquakes ($M_s = 5.5$

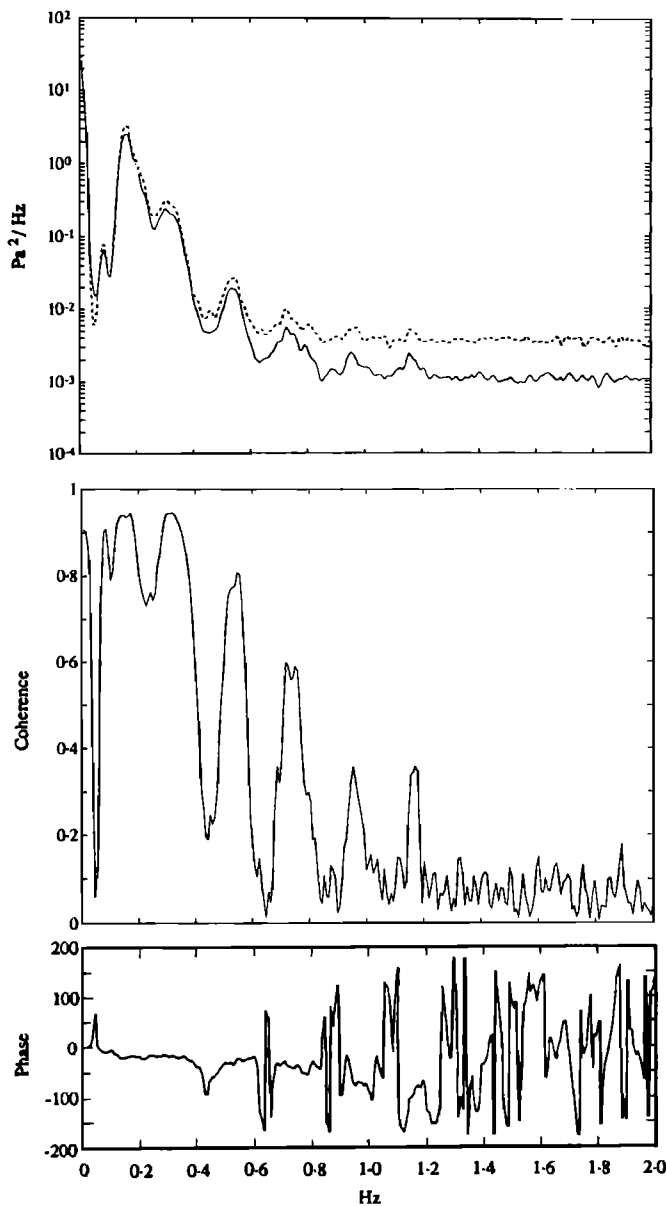


FIG. 4. Pressure spectra (top panel), coherence (middle), and phase (lower) between instruments "red" and "white" during one, 4-h record. The spectrum from the instrument red (dashed) is slightly noisier than the spectrum from white (solid line). Peaks within the pressure spectrum correspond to bands of high coherence between instruments. The small phase lags detected within the peaks suggest propagation nearly broadside to the array.

and $M_s = 6.9$) near Costa Rica on 25 March 1990. This event occurs in the interval near 192 h in Figs. 5 and 6. The seafloor measurements are dominated by the Rayleigh surface wave component. In contrast, the measurements of Keenan and Dyer,²¹ using near surface hydrophones under the ice show primarily the water borne "T" phase component. These earthquake wave trains will be discussed in greater detail in a future paper.

IV. MODELING THE SHAPE OF THE MICROSEISM PEAK

The series of evenly spaced troughs and peaks across the microseism peak in the Arctic measurements must be related

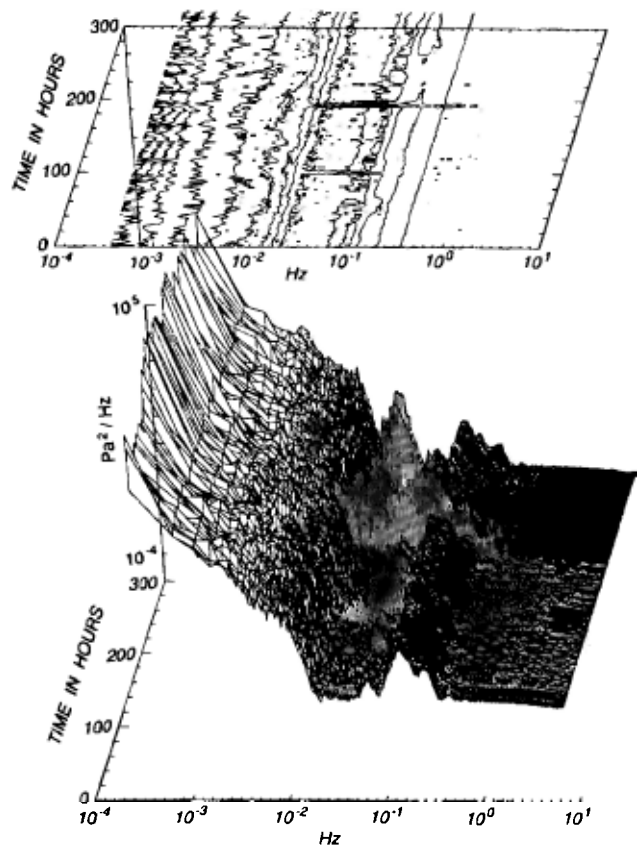


FIG. 5. Contour and mesh plots showing the evolution of the pressure spectrum measured with instrument "green" during the experiment. The stability of the shape and amplitude of the microseism peak is evident. The wave trains from several large earthquakes generate transitory broad peaks centered around a 25-s period.

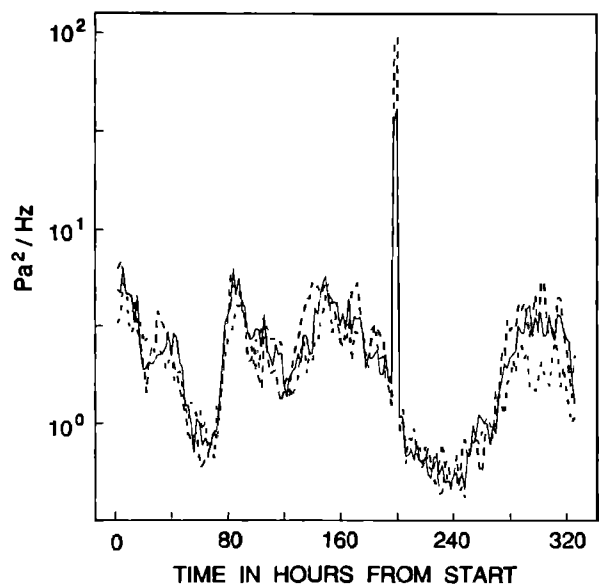


FIG. 6. Spectral density in three bands near 0.15 Hz versus time in hours from the start of the experiment. The energy in this peak in the microseism band varies by 10 dB over the 2 week period. The peak at 192 h is caused by the wave trains from a pair of large earthquakes.

to the modes of propagation in the ocean-rock waveguide of the Arctic ocean. The simplest model of an ocean waveguide with a pressure release surface and a reflecting bottom leads to a series of modes existing within a frequency range bounded below by the frequencies:

$$f_n = (n + \frac{1}{2})(c/2h); \quad n = 0, 1, 2, \dots,$$

where h is the water depth and c is the speed of sound (Fig. 7). These are the quarter wave and higher resonances of the waveguide. The water depth (h) at the Beaufort site is 3400 m, so the cutoff frequencies are at 0.11, 0.33, 0.55, 0.77 Hz, etc. The relationship between these frequencies and the peaks in the seafloor pressure spectrum seems apparent. In this model, the group velocity of each mode approaches zero near the cutoff frequency. A simple model of modes propagating in water of varying depth would require peaks in the spectrum associated with minimums in the group velocity to maintain a constant energy transport.

The modal structure becomes very complex in a more realistic ocean model. The structure of the Beaufort seafloor includes from 4 (Ref. 22) to 8 km of sediment.²³ The soft sediment profoundly affects the character of the modes of the oceanic waveguide.²⁴ Figure 7 displays the phase velocities of the first 20 Rayleigh modes in a model for this site in the Beaufort Sea. The phase velocity curves for the first four modes in the rigid seafloor model are shown dashed. At these low frequencies there are no distinct ocean waveguide acoustic modes; rather the ocean is just part of a much larger waveguide involving the ocean, sediments, and rocks of the crust and upper mantle. The density of modes at acoustic velocities near 1.5 km/s is increased threefold by the presence of the deep sediment layer in comparison to the rigid seafloor model. At these low frequencies the usual ocean waveguide associated with the ocean sound velocity minimum is unimportant. The ocean, sediments, and mantle rocks have very different compressional and shear velocities so that each acts like a waveguide with a characteristic mode type. This concept is only approximate and a real mode in this complicated set of waveguides will involve energy prop-

agating in all layers. Figure 7 shows evidence for these three interconnected waveguides. Rayleigh modes propagate at mantle shear velocities (3.5 + km/s), and generate displacements at great depth. The ocean and seafloor form the second waveguide; modes propagate essentially as acoustic waves in the ocean (1.5–3.5 km/s). The third set of modes propagate as shear modes in the sediments (< 1.5 km/s). These three types of waves merge together into a single set of dispersion curves. The character of each mode may change abruptly with small changes in frequency along the dispersion curve.

Previous work on mode propagation on the seafloor has suggested that often the energy at any particular frequency in the microseism peak will be associated almost exclusively with a single mode. There is usually only a narrow band of frequencies for which a mode will propagate at phase velocities between 1.5 and 3 km/s. Microseisms are excited by processes at the ocean surface. The eigenfunctions of the faster modes are largest at deeper depths, and are more weakly excited than slower traveling components.^{1,25} Waves traveling at speeds less than the speed of sound in water (1.5 km/s) have eigenfunctions that are evanescent from the seafloor in both directions. The slowest modes are weakly excited by sources at the sea surface and also experience significant dissipation because of the localization of energy within the sediment layer. These "Stoneley" modes may be generated by scattering at the rough rock-sediment boundary and so become an important component of seafloor noise, but the evidence is inconclusive.²⁵ At the Arctic seafloor site scattering processes are probably insignificant because of the great depth of the sediments. In shallow (shelf depths) water the Stoneley modes are directly excited by the surface sources and dominate the microseism spectrum.²⁶

The phase velocity curves for the modes in the Beaufort Sea model are approximately coincident to the rigid seafloor model phase velocity curves at some frequencies at phase velocities near the speed of sound in water (1.5 km/s). Chiaruttini *et al.* have shown that the eigenfunctions for the modes in a complex (more complete) model will resemble the eigenfunctions derived from a simpler model in frequency bands for which the phase velocity curves for the two models are nearly coincident.²⁷ In the frequency band from 0.1 to 0.2 Hz, the eigenfunction for the third mode in the realistic ocean model should resemble the eigenfunction for the simple rigid seafloor model, with most of the energy associated with acoustic energy in the ocean (Fig. 8). This resemblance is limited to the band in which the phase velocity curves coincide; the eigenfunctions are very different at frequencies outside of the band. We suggest these "pseudoacoustic" modes are associated with the regular sequence of peaks and troughs in the Arctic seafloor pressure spectra.

One hypothesis is that the peaks in the Arctic spectrum are associated with the reflection and transmission of, or coupling between Rayleigh modes at the continental shelf. This problem has been extensively studied, but only at frequencies below the microseism peak.²⁸ It may be feasible to calculate coupling coefficients for down slope propagation of Rayleigh waves²⁹ but this is beyond the scope of this paper. The mode coupling problem in the purely acoustic case

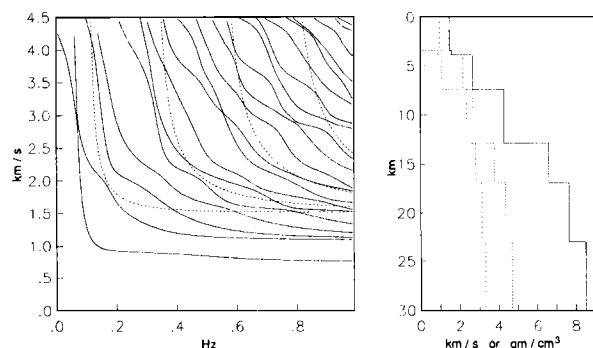


FIG. 7. (Left) phase velocity for the 20 Rayleigh wave modes in a realistic model for the ocean and seafloor at the Arctic site. Also shown (dashed) phase velocity for modes in a model ocean with a rigid seafloor. (Right) model used in the modal calculations based roughly on Baggereor and Falconer;²² compressional velocity (solid), shear velocity (short dash), and density (long dash). The seafloor is at 3.4-km depth.

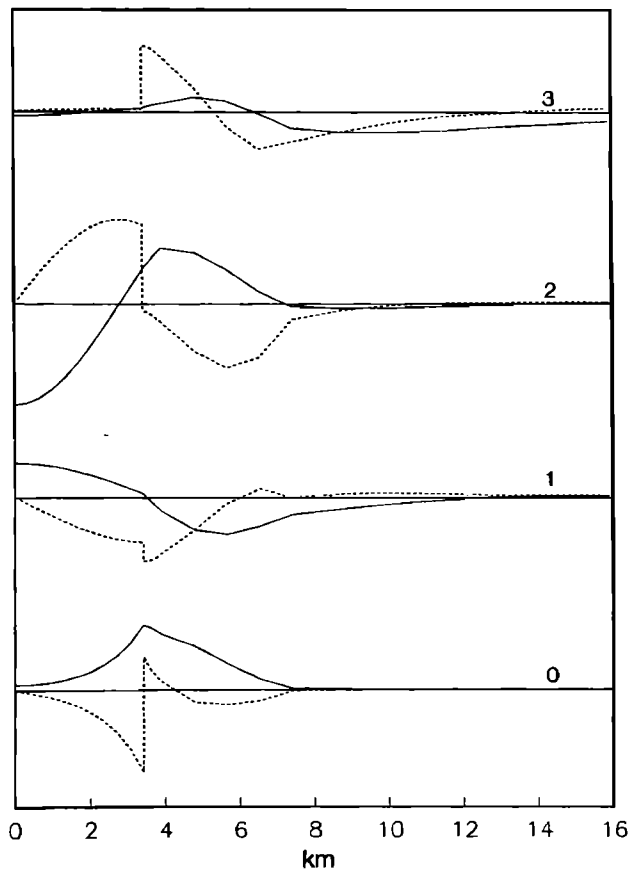


FIG. 8. Vertical (solid) and horizontal (dashed) eigenfunctions for the first four modes at 0.125 Hz. The eigenfunction for the third mode resembles the fundamental mode eigenfunction in a model ocean with a rigid seafloor since there is a cosine dependence with depth for the vertical velocity with a zero crossing near the seafloor, and a sine dependence for the horizontal component with a maximum at the seafloor. The fundamental mode in this model is a Stoneley wave with an exponential decay of the eigenfunction away from the seafloor. The fourth mode is essentially a pure Rayleigh wave within the rock.

is still complicated.⁴⁰ We have collected seismic data at a station in Prudhoe Bay, Alaska, south of the deployment site and will be comparing this record of microseisms against the seafloor measurements to look at the transmission of microseisms across the shelf.

A second hypothesis, as suggested earlier, is that the peaks in the spectrum are associated with maintaining a constant energy flux as the group velocity and eigenfunction of each mode varies during propagation downslope (adiabatic modes). To examine these two possibilities we use a simple model of a source at the shelf edge (modeling the elastic wave energy propagating across Alaska) and propagate the signal down slope to the site. The model is two dimensional, with no variation along shore. One set of calculations uses an ocean of constant depth (3.4 km). The ocean floor just beyond the continental shelf north of Alaska lies at a depth of about 2.5 km. A second set of calculations starts the modes at 2.5-km depth and propagates the modes adiabatically to the site at 3.4-km depth.

The first problem is to model the excitation of the modes at the shelf edge. A Rayleigh wave in a half-space has an eigenfunction that decays away from the free surface exponentially. The wave number and frequency spectra of microseisms measured midcontinent with the LASA array show most of the energy is in the fundamental mode Rayleigh wave at long period and in higher-order modes at frequencies between 0.2 and 0.3 Hz, and in compressional waves at higher frequencies.³¹ We model the fundamental mode incident at the shelf edge as a displacement of a vertical wall in the ocean layer, and evade the question of the exact character of microseisms on land. The displacement decays exponentially with depth with an *e*-folding distance equal to 3.5 km/s divided by the radian frequency. This velocity is characteristic of fundamental and higher modes on land in this frequency band. A simpler source model (a vertical line force at the sea surface) generated similar results. The frequency spectrum of the source is assumed to be white (constant in frequency), and the third dimension parallel to the coast is established by extending the source to infinity in the direction along the coast (no dependence in the along-shore direction).

We use a Green's function technique to determine the excitation of modes. Following the notation of Aki and Richards,³² the pressure signal at the seafloor at a point (x_0, z_0) due to a point force of amplitude f at (x, z) with harmonic time dependence can be written as a sum over the mode Green's functions:

$$p(x_0, z_0, t) = f e^{i\omega t} \sum_n G_n(x_0, z_0; x, z; \omega);$$

for a horizontal point force:

$$G = [u(z)p(z_0)/4\omega UI_1] J_0(k|x_0 - x|),$$

where u and p are the horizontal displacement and pressure field associated with each mode. The group velocity is U . I_1 is an integral over depth of the density weighted sum of the squares of the displacements and proportional to the kinetic energy density in each mode. We model the Rayleigh waves propagating across Alaska from the Pacific ocean associated with this distant microseism source as a line source along a vertical wall representing the shelf edge. The pressure signal at a distance away from the coast can be predicted by integrating in depth the Green's function times a model of the vertical dependence of the source, in this case an exponential function with a characteristic scale.

The second part of the problem is to model the changing mode amplitudes as the waves propagate from near the shelf into deeper water off-shore. Here, we use adiabatic mode propagation arguments. The amplitude of the modes is adjusted to maintain constant energy transport from shallow to deep water, and the mode eigenfunction is reevaluated at the water depth appropriate for the receiver location. We assume the phase between modes becomes random some small distance from the coast so that the power in each mode can be added together to determine the pressure spectrum at the receiver.

Figure 9 shows the results of these calculations. The remarkable resemblance of the model spectrum to the measured spectrum despite no frequency dependence of the

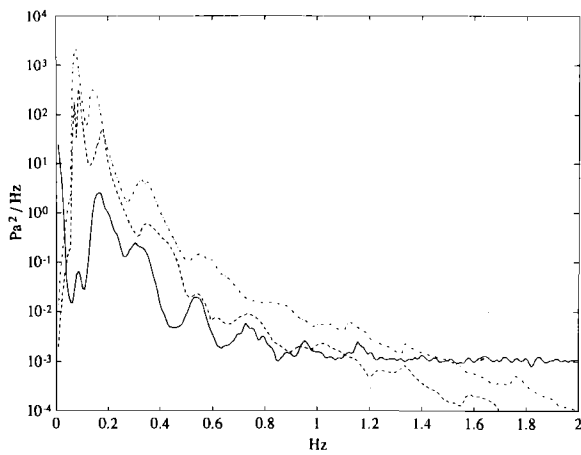


FIG. 9. Typical spectrum from the Arctic seafloor (solid line). Results from modeling the excitation of modes at the shelf break in an ocean of constant depth (dash-dot line) and in an ocean where the depth varies from a depth of 2.5 km at the source to 3.4 km at the observation point (dashed).

source demonstrates the importance of modes in determining the spectral shape. The amplitude of the single frequency peak at 0.08 Hz is much too large compared to the amplitude of the double frequency microseisms at 0.11 Hz, but otherwise the predicted amplitudes for the various peaks appear correct. The single frequency energy detected at continental sites is usually 20 to 30 dB smaller than the double frequency peak since the mechanism creating the single frequency peak is very different from the double frequency mechanism. The shear modulus of the near surface sediments is important in determining the amplitude of the peaks and troughs in the spectrum; the peaks disappear if the shear modulus is very small. The pseudoacoustic modes should look more like acoustic modes over a rigid bottom when the seafloor is more rigid. This result is in agreement with the view that the pseudoacoustic modes are associated with the periodicities in the spectrum. The locations of the peaks in the model fit the observations only poorly, but the character of the spectrum is well modeled. This component of the modeling suggests that it is the coupling of the energy at the shelf break into waveguide modes that determines the shape of the spectrum.

The fit can be greatly improved by changing the water depth in the model, perhaps accounting for changes in the mode amplitudes and eigenfunctions during propagation toward deeper water. The second curve shows the results from propagating the source from water of 2.5-km depth (just beyond the shelf) out to the site in 3.4 km of water, maintaining a constant energy flux. The peaks at 0.7 and 0.9 Hz now match up, suggesting the higher-order peaks are associated with this second process of maintaining the energy flux as the position (in frequency) of the minimums of the group velocity curves for each mode shifts with the changing water depth. Our modeling efforts suggest that it is not possible to model the location in frequency of these higher-order peaks, without either changing the water depth in the model (to 4-km depth) or else by allowing for propagation of modes down slope.

V. COHERENCE IN THE MICROSEISM BAND

The coherence between pairs of instruments shows peaks and troughs that correspond to the peaks in the power spectrum (Fig. 4). The coherence is apparently mostly controlled by the signal-to-noise ratio of the measurements. Coherences measured between the more closely separated instruments are similar, except some instruments are noisier than others. This measurement of the coherence contrasts greatly with measurements between closely spaced instruments on the Pacific seafloor. Instruments separated by 2 km on the Pacific seafloor are incoherent above 0.2 Hz.¹⁰ Schreiner and Dorman suggest scattering of energy from Rayleigh modes into Stoneley (sediment) waves controls the coherence observed across a very small (150-m aperture) seafloor array of seismometers. They observe a very different structure to the coherence than is seen in the Arctic measurements.²⁵

In this record, the phase difference between the “white” instrument and either the “blue” or “green” instruments is very small ($< 5^\circ$) in the band from 0.1 to 0.7 Hz (the band for which the coherence is significantly different from zero for these pairs of instruments). The small phase differences observed suggest propagation nearly broadside to the array. We will assume a propagation velocity near 1.5 km/s consistent with oceanic Rayleigh modes above 0.2 Hz. Larger phase velocities are possible that would suggest larger angles between the direction of propagation and the orientation of the array. We infer the direction of propagation of these waves must be from either about 15° (true), suggesting we are seeing energy that has propagated across Alaska from the stormy Gulf of Alaska or from about 200° (true) and from the Norwegian Sea. The uncertainties in the timing of the instruments and the errors in the phase measurements preclude differentiating between the two azimuths.

Wave-number spectra generated from data from several large continental seismic arrays suggest microseism energy is primarily associated with surface wave modes.³³ These studies also identified the Gulf of Alaska as a common source for microseisms. We cannot rule out energy associated with body waves; body waves from distant sources propagate at velocities greater than 7 km/s, and would generate little phase lag across the array.

The coherence between the red and white instruments is above 0.95 in the spectral peaks below 0.4 Hz. At low frequency we would expect to see essentially perfect coherence between instruments, because the wavelengths of Rayleigh waves are so long (30 km at periods near 10 s). The coherence in each of the spectral peaks allows us to put upper bounds on the beamwidth of these signals. Signals from varied directions add incoherently (in the absence of scattering effects), so the coherence is less between instruments in a wave field with a broader distribution of propagation directions. The constraint on the beamwidth is weak at low frequency, because the wavelengths of the signals are large compared to the distance between the instruments and the phase differences are small. We model the microseism wave field as a single mode with a phase speed of 1.5 km/s, a directional spectrum that is uniform within an angle 2ϕ , and zero outside this angle, and ask what the behavior of the

coherence is as a function of frequency and the half beam-width parameter ϕ (Fig. 10). The figure shows the coherence corresponding to the frequencies 0.1, 0.25, 0.5, and 1.2 Hz. At 0.1 Hz, the observation that the coherence is above 0.9 does not constrain the directional spectrum at all. At 0.25 Hz, a coherence of 0.95 constrains the half-width angle to less than 30° , at 0.5 Hz, a coherence of 0.8 requires a half-width angle of less than 15° , and at 1.18 Hz, a coherence of 0.35 constrains the half-width to be less than about 12° . Since we believe the coherence is reduced by electronic noise, we infer from these calculations, that the energy in the microseism peak is propagating from a narrow range of directions at least at frequencies above 0.5 Hz. This is consistent with one large, distant source (in the Gulf of Alaska). The low energy throughout the spectrum is also consistent with distant sources, and indeed the coherences observed preclude significant local sources (which would tend to make the wave field more isotropic).

VI. VERY LOW FREQUENCY WAVES

The energy in the pressure spectra from the Arctic seafloor increases rapidly at periods longer than about 50 s (Fig. 3). Pressure spectra from sites on the floor of both the Atlantic and the Pacific show a similar rapid rise in spectral levels at long periods, but the spectra from the three oceans differ in subtle, but important ways. The Arctic spectrum is between 20 and 30 dB quieter than a typical spectrum from the Pacific at frequencies near 0.01 Hz and about 10 dB lower than typical spectra from an Atlantic site. However, the spectra are more similar in amplitude at frequencies below 0.001 Hz suggesting some mechanism to maintain a uniform spectral level at these very low frequencies (Fig. 3).

Are the pressure signals we see at the seafloor related to measurable displacements of the surface of the ice? Gravity-meter measurements of vertical displacement can be associated with propagating waves in the ice.^{11,13} The properties

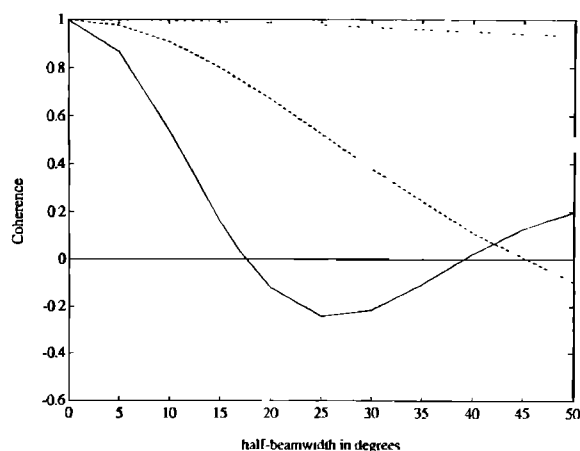


FIG. 10. Coherence versus beam width and frequency between instruments 1.5 km apart. Model assumes a uniform directional distribution within an angle 2ϕ , and no energy outside the angle. Coherence shown for four frequencies (0.1, 0.25, 0.5, and 1.1 Hz). Coherence is nearly independent of beamwidth at low frequency.

of waves in ice over water (flexural-gravity waves) are well understood. At short periods the rigidity of the ice determines the phase speed. At long periods, the waves are essentially identical to normal ocean waves.^{13,34} There is a local minimum in the group velocity for waves on typical arctic ice (thickness 2.5 m) between a 20- and 35-s period and the on-ice gravity-meter measurements show a peak in the acceleration spectrum in the same band. The rms displacement in the band from 0.01 to 0.05 Hz is a few tenths of a millimeter. Hunkins was able to demonstrate phase propagation near a 35-s period at about 38 m/s.¹³

The pressure signal from ocean waves or from coupled ocean-ice waves attenuates with depth with an e -folding scale equal to the inverse wave number. Pressure spectra measured at sites on the seafloor of both the Pacific or the Atlantic are energetic at very long period, with a precipitous decrease above a corner frequency which depends only on the water depth above the site.^{1,10} This frequency corresponds to a wave number equal to the inverse water depth. The water depth over the instruments in the Arctic was about 3400 m, and the corner frequency about 0.0075 Hz. The Arctic pressure spectra do appear to exhibit a more rapid fall with increasing frequency above 0.008 Hz, although the spectrum is always very "red" in this low-frequency band. The presence of the ice introduces a negligible change in the corner frequency for this water depth. Below the corner frequency, we can infer the sea surface displacements corresponding to the arctic floor pressure signals directly. One Pascal in pressure corresponds to 0.1 mm of surface displacement. LeSchack and Haubrich measured displacement spectral densities at 0.01 Hz between 3 and 10 mm^2/Hz .¹¹ Our measurements of the pressure spectrum show values near 50 Pa^2/Hz at 0.01 Hz corresponding to displacement spectral densities after correcting for the decay from the surface of about 1 or 2 mm^2/Hz . The on-bottom pressure measurements in this band are consistent with displacement measurements made 30 years ago. The measurements of LeSchack and Haubrich do not extend further in frequency so we are unable to compare the surface and bottom measurements at a longer period.¹¹

There have been several recent measurements of tilting and straining of the ice in the Arctic. The spectra of both tilt and horizontal strain exhibit a broad peak near a 35-s period.^{14,15} A persistent, small bump, or ledge in the Arctic pressure spectrum near 50 to 60 s in period, may be the seafloor manifestation of this peak, obscured by the hydrodynamic filtering. We can use the flexural-gravity wave dispersion relation to predict the pressure signal from the strain and tilt measurements. Figure 11 shows the relationship between the tilt spectrum in the direction of propagation and the pressure spectrum. The figure shows two curves, one relating the tilt to pressure fluctuations near the sea surface and the second to pressure fluctuations at the seafloor. The pressure signal at the seafloor at periods shorter than 50 s is much reduced because of the hydrodynamic "filtering" above the corner frequency. Estimates of the seafloor pressure spectrum at four frequencies associated with the tilt spectrum measured by Czipott and Podney on the ice near Greenland are plotted in Fig. 3. The tilt measurements predict very similar ampli-

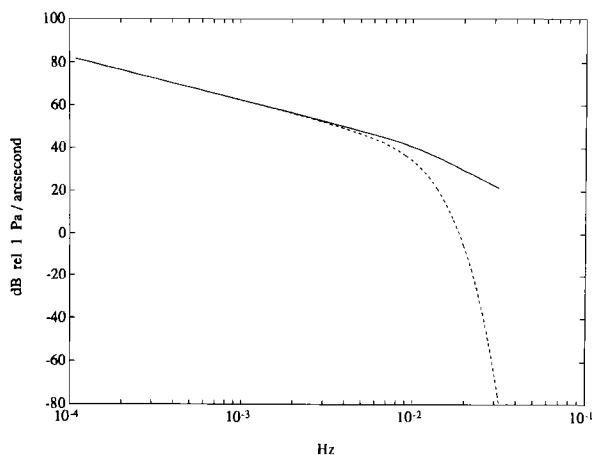


FIG. 11. Conversion from a spectrum of tilt to a pressure spectrum at the sea surface (solid) and the seafloor (dashed). Units are in dB relative to 1 Pa/arcsecond.

tudes for the flexural-gravity waves as do the pressure measurements. The authors report the tilt measurements have a large uncertainty in calibration. The strain measurements appear much noisier than the tilt measurements in the flexural-gravity wave band. The relationship between horizontal strain and the amplitude of the flexural gravity waves is complicated because it depends on the elastic parameters in the ice, and the thickness of the ice.¹⁴ The strain measurements predict larger flexural-gravity wave amplitudes at long periods than the tilt measurements. It appears that the strain spectrum may depend on other physical processes such as deformation by the wind and internal waves.

Our understanding of these waves requires an explanation for the very similar amplitudes seen in the Norwegian-Greenland Sea and the Beaufort Sea and the small variability in amplitude from day to day. We see only a factor of 2 variability in energy in the long wave band (Fig. 12). There are three possibilities: (1) the loss during propagation is so slight that the two areas see the same wave field, (2) there is a universal source such as the force of wind on the ice, that generates and maintains a uniform level, and (3) inadequate data has failed to identify the true variability in the wave field.

Hunkins related the waves he detected to forcing by the local wind.¹³ Haubrich and LeSchack reexamined this problem and found little variation in the spectrum of ice displacement between windy and calm days.¹¹ They concluded that forcing by local winds was of secondary importance and that the long period energy they saw had propagated in from the open ocean. Squire measured the oscillations of the ice on a lake under the influence of the wind.³⁵ We see no correlation between the local surface winds measured at the ice camp and the pressure record below 0.01 Hz (Fig. 12). The amplitude varies about a factor of 2 over the 2-week period. Czippott and Podney also found no correlation between the local wind and ice tilts, and suggested the ice is usually too thick to respond to local wind forcing with other than essentially static deformation.¹⁴ Propagation directions inferred from

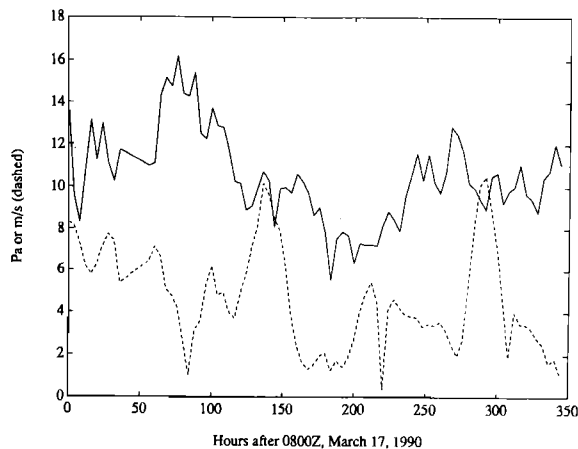


FIG. 12. Root-mean-square pressure signal between 0.001 and 0.03 Hz versus time, in 4-h segments. Also shown (dashed) the wind velocity measured at the APLIS ice camp over the same interval.

the tilt measurements suggested propagation through the ice from the open sea.

Webb *et al.* have shown a relationship between pressure fluctuations on the seafloor of the western Atlantic and the average short period wave height along the shore of the central Atlantic.¹⁰ The model suggests a conversion from short-to long-period energy in the surf zone by nonlinear mechanisms. The long-period energy then propagates to deep water as free waves.

The ice is no barrier to these very long-period waves, however it is difficult to reconcile the similar amplitudes detected in the Beaufort and Greenland Seas, given the constricted geometry of the Arctic ocean straits. These long waves are only gently steered by bathymetry. The Norwegian Sea and the Beaufort Sea are not connected by a great circle path, the approximate propagation path for a long wave. Energy that has reached the Beaufort from the Atlantic must have either reflected from a shore line, or scattered from topography. Reflection of long-surface gravity waves from coastlines is usually not very efficient.¹⁰ We are considering whether another process that might generate long-period waves may be the action of atmospheric pressure fluctuations in shallow water. Wind can generate large-scale oscillating pressure fluctuations that propagate with the wind velocity. The phase velocity of long-period waves can be comparable to wind velocities in shallow water. This idea will need to be tested during a subsequent experiment.

VII. CONCLUSIONS

We have measured the amplitude of the pressure spectrum at the floor of the Beaufort sea in the frequency band from 0.0001 to 8 Hz. We found very quiet levels across the entire band. Both single- and double-frequency microseism peaks are obvious throughout the experiment. The microseism spectrum is remarkably stationary over 2 weeks. The double-frequency peak is subdivided into a least five peaks apparently associated with the propagation of individual

seismoacoustic modes. The energy in the microseism peak is very coherent across the band. The phase relationship between instruments suggests a direction of propagation of about 15° (true) from a wide source region in the Gulf of Alaska. Large earthquakes generate wave trains that occasionally dominate the pressure spectrum at all frequencies. The earthquake spectra are peaked at about a 25-s period.

At periods longer than 50 s, the spectrum rises abruptly because of pressure fluctuations caused by freely propagating gravity waves. The pressure measurements suggest wave heights similar in amplitude to that predicted from ice surface gravimeter and tilt measurements. The speculation in the literature suggest this long period energy propagates in from the open sea. Another possibility is wind forcing, possibly occurring primarily in shallow water. More work will be required before the source of long-period flexural-gravity waves in the Arctic is unambiguously identified.

ACKNOWLEDGMENTS

This work was supported by the Office of Naval Research (N00014-90-J-1088, and UW Subcontract 721907). We thank the crew of the APLIS ice station for their cheerful assistance with the instrument deployments. Brian Lewis provided comments on the first draft, and Luciana Astiz assisted with data analysis. Thanks also to J. Lemire and T. Deaton, the builders of the instruments used in the Arctic.

- ¹ S. C. Webb and C. S. Cox, "Observations and modeling of seafloor microseisms," *J. Geophys. Res.* **91**, 7343-7358 (1986).
- ² G. H. Sutton and N. Barstow, "Ocean bottom ultralow frequency (ULF) seismo-acoustic ambient noise, 0.002 to 0.4 Hz," *J. Acoust. Soc. Am.* **87**, 2005-2012 (1990).
- ³ K. A. Hasselmann, "A statistical analysis of the generation of microseisms," *Rev. Geophys. Space Phys.* **1**, 177-210 (1963).
- ⁴ B. M. Buck and J. H. Wilson, "Nearfield noise measurements from an Arctic Pressure ridge," *J. Acoust. Soc. Am.* **80**, 256-264 (1986).
- ⁵ A. R. Milne, J. H. Ganton, and D. J. McMillan, "Ambient noise under sea ice and further measurements of wind and temperature dependence," *J. Acoust. Soc. Am.* **41**, 525-528 (1967).
- ⁶ N. C. Makris and I. Dyer, "Environmental correlates of pack ice noise," *J. Acoust. Soc. Am.* **80**, 1434-1440 (1986).
- ⁷ J. K. Lewis and W. W. Denner, "Arctic ambient noise in the Beaufort Sea: seasonal space and time scales," *J. Acoust. Soc. Am.* **82**, 988-991 (1987).
- ⁸ J. K. Lewis and W. W. Denner, "Arctic ambient noise in the Beaufort Sea: seasonal relationships to sea ice kinematics," *J. Acoust. Soc. Am.* **83**, 549-565 (1988).
- ⁹ D. D. Prentiss and J. I. Ewing, "The seismic motion of the deep ocean floor," *Bull. Seism. Soc. Am.* **53**(4), 765-781 (1963).
- ¹⁰ S. C. Webb, X. Zhang, and W. Crawford, "Infragravity waves in the deep ocean," *J. Geophys. Res.* **96**(2), 2723-2736 (1991).
- ¹¹ L. A. LeSchack and R. A. Haubrich, "Observations of waves on an ice-covered ocean," *J. Geophys. Res.* **69**(18), 3815-3821 (1964).
- ¹² A. P. Crary, R. D. Lotell, and J. Oliver, "Geophysical studies in the Beaufort Sea, 1951," *Trans. Am. Geophys. U.* **33**(2), 211-216 (1952).
- ¹³ K. Hunkins, "Waves on the Arctic Ocean," *J. Geophys. Res.* **67**(6), 2477-2489 (1962).
- ¹⁴ P. V. Czipott and W. N. Podney, "Measurements of fluctuations in tilt of Arctic ice at the CEAREX Oceanography camp: experimental review, data catalog and preliminary results," Final Tech. Rep. PD-LJ-89-369R, p. 53, Physical Dynamics, Inc., La Jolla, CA, 1989.
- ¹⁵ R. S. Williams, S. Moore, P. Wadhams, and M. Beard, *Measurements of Strain in Sea Ice during FRAM 3* (Scott Polar Research Institute, Cambridge, 1989), Vol. 89-1.
- ¹⁶ C. S. Cox, T. K. Deaton, and S. C. Webb, "A deep sea differential pressure gauge," *J. Atm. Oceanic Tech.* **1**(3), 237-246 (1984).
- ¹⁷ S. C. Webb, "Long period acoustic and seismic noise and ocean floor currents," *IEEE J. Oceanic Eng.* **13**, 263-270 (1988).
- ¹⁸ S. C. Webb, "Very low frequency sound studied using multielement seafloor arrays," in *Proceedings of Natural Physical Sources of Underwater Sound*, edited by B. Kerman (Cambridge U.P., Cambridge, 1990) (in press).
- ¹⁹ H. Kutschale, "Arctic hydroacoustics," *Arctic* **22**, 247-264 (1969).
- ²⁰ A. C. Kibblewhite and K. C. Ewans, "Wave-wave interactions microseisms and infrasonic ambient noise in the ocean," *J. Acoust. Soc. Am.* **78**, 981-994 (1985).
- ²¹ R. E. Keenan and I. Dyer, "Noise from Arctic ocean earthquakes," *J. Acoust. Soc. Am.* **75**, 819-825 (1984).
- ²² A. B. Baggereor and R. Falconer, "Array refraction profiles and crustal models of the Canada Basin," *J. Geophys. Res.* **87**(B7), 5461-5476 (1982).
- ²³ B. L. N. Kennett, "Guided wave attenuation in laterally varying media," *Geophys. J. Int.* **100**, 415-422 (1990).
- ²⁴ G. F. Panza, "Synthetic seismograms: the Rayleigh waves model summation," *J. Geophys.* **58**, 125-145 (1985).
- ²⁵ A. E. Schreiner and L. M. Dorman, "Coherence length of seafloor noise: effect of ocean bottom structure," *J. Acoust. Soc. Am.* **88**, 1503-1514 (1990).
- ²⁶ H. Schmidt and W. A. Kuperman, "Estimation of surface noise source level from low frequency seismoacoustic ambient noise measurements," *J. Acoust. Soc. Am.* **84**, 2153-2162 (1988).
- ²⁷ C. Chiaruttini, G. Costa, and G. F. Panza, "Wave propagation in multi-layered media: the effect of waveguides in oceanic and continental earth models," *J. Geophys. Res.* **58**, 189-196 (1985).
- ²⁸ L. A. Drake and B. A. Bolt, "Finite element modeling of surface wave transmission across regions of subduction," *Geophys. J. Int.* **98**, 271-279 (1989).
- ²⁹ B. L. N. Kennett, "Guided wave attenuation in laterally varying media," *Geophys. J. Int.* **100**, 415-422 (1990).
- ³⁰ W. A. Kuperman, M. B. Porter, and J. S. Perkins, "Rapid computation of acoustic fields in three-dimensional ocean environments," *J. Acoust. Soc. Am.* **89**, 125-144 (1991).
- ³¹ R. T. Lacoss, E. J. Kelly, and M. N. Toksoz, "Estimation of Seismic Noise Structure Using Arrays," *Geophysics* **34**(1), 21-38 (1969).
- ³² K. Aki and P. G. Richards, in *Quantitative Seismology Theory and Methods* (Freeman, San Francisco, 1980), p. 303.
- ³³ R. K. Cessaro and W. W. Chen, "Wide-angle triangulation array study of simultaneous primary microseism sources," *J. Geophys. Res.* **B11** 15555-15563 (1989).
- ³⁴ J. W. Davys, R. J. Hosking, and A. D. Sneyd, "Waves due to a steadily moving source on a floating ice plate," *J. Fluid Mech.* **158**, 269-287 (1985).
- ³⁵ V. A. Squire, "Wind over ice: a mechanism for the generation of ice-coupled waves," in *Ice Technology, Proceeding of the 1st International Conference* (Springer-Verlag, Berlin, 1986), pp. 115-127.